

FRP Repair of Corrosion-Damaged Reinforced Concrete Beams

Khaled A. Soudki, Ted Sherwood, and Sobhy Masoud

Department of Civil Engineering
University of Waterloo, Waterloo, Canada

Abstract

Corrosion of steel reinforcement is one of the main durability problems facing reinforced concrete infrastructures worldwide. This paper will summarize the results of a multi-phase experimental program undertaken at the University of Waterloo to investigate the viability of using externally bonded fiber reinforced polymer (FRP) laminates to rehabilitate corrosion-damaged reinforced concrete beams. Several reinforced concrete beams with variable chloride levels (0 to 3%) were constructed. The beams were strengthened or repaired by externally epoxy bonding FRP laminates to the concrete surface. The tensile reinforcement of the specimens was subjected to accelerated corrosion by means of impressed current up to 15% mass loss. Strain gauges were used on the FRP laminates to quantify tensile strains induced by the corrosion process. Following the corrosion phase, the specimens were tested in flexure in a four-point bending regime. Test results revealed that FRP laminates successfully confined the corrosion cracking and spalling due to expansion of corrosion products. The FRP strengthened beams exhibited increased stiffness over the unstrengthened specimens, and marked increases in the yield and ultimate strength. The results showed that the use of FRP sheets for strengthening corroded reinforced concrete beams is an efficient technique that can maintain structural integrity and enhance the behavior of such beams.

Key words: CFRP laminates, corrosion, confinement, expansion, load tests, strengthening, bond strength, reinforced concrete.

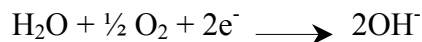
Introduction

Corrosion of reinforcing steel is a major problem facing the concrete infrastructure. Many structures in adverse environments have experienced unacceptable loss in serviceability or safety far earlier than anticipated due to the corrosion of reinforcing steel and thus need replacement, rehabilitation, or strengthening. Corrosion presents a problem for reinforced concrete (RC) structures for two reasons. First as steel corrodes, there is a corresponding drop in the cross-sectional area. Secondly, the corrosion products occupy a larger volume than the original steel which exert substantial tensile forces on the surrounding concrete and causes it to crack and spall off. The expansive forces caused by steel corrosion can cause cracking, spalling and staining of the concrete, and hence loss of structural bond between the reinforcement and concrete (ACI Committee 222 1996). A heavily corroded RC member tends to fail due to loss of bond and bond splitting. This implies that if corrosion cracking can be prevented or delayed, a certain degree of structural strength may be maintained in a corroding RC beam.

The degree of corrosion is considered as one of the main parameters to predict the useful service-life of corroding reinforced concrete structures. It is possible, with varying degrees of accuracy, to measure the amount of steel dissolving and forming oxides (rust). This is done directly as a measurement of the electric current generated by the anodic reaction;



and consumed by the cathodic reaction;



and then converting the current flow by Faraday's law to metal loss;

$$\Delta m = MIt/zF$$

Where Δm is the mass of steel consumed (g), M is the atomic weight of metal (56 g for Fe), I is the current (Amperes), t is the time (Seconds), z is the ionic charge (2), and F is Faraday's constant (96500 Amperes. Seconds).

Fibre reinforced polymer (FRP) systems are promising alternatives for the rehabilitation of deteriorated and deficient concrete members. In addition to their high strength to weight ratio, durability in adverse environments and high fatigue strength, FRP sheets can be easily externally bonded to reinforced concrete slabs, beams, and columns (ACI Committee 440 1996). The use of fibre reinforced polymer (FRP) laminates for the rehabilitation and strengthening of corrosion-damaged infrastructure is very recent. Many researchers have attempted to characterize the performance of corrosion-damaged RC structures but little information is available in the literature on the structural behaviour of such beams strengthened or repaired with FRP sheets. The author and his research group are attempting to fill this gap in the literature (Masoud and Soudki 2000, 2001, Sherwood and Soudki 1998, 1999, 2000; Soudki and Sherwood 1998, 2000; Soudki et al. 2000; Soudki 1999). It can be hypothesised that an FRP wrapped member undergoing active corrosion may exhibit improved structural performance by a combination of the following two mechanisms: 1) confinement of the concrete section, thereby lessening corrosion cracking and bond splitting cracks, 2) prevention of further chloride ingress into concrete, thereby reducing rate of corrosion, and 3) increased flexural and shear resistance to overcome the loss in the steel cross-section.

This paper highlights the research findings of a multiphase experimental study aimed to examine the viability of using FRP wraps to strengthen or repair reinforced concrete beams subjected to corrosion damage.

Test Program

The overall program included 16 small-scale reinforced concrete beams (100×150×1200mm), 9 medium-scale beams (175×125×2000mm) and 20 larger-scale beams (152×254×3200). This paper will present on the monotonic test results from the small- and large-scale reinforced concrete beams.

Figure 1(a) shows the reinforcement details of the small-scale specimens. It consisted of two No.10 Grade 400 tensile reinforcement, two 6-mm diameter Grade 400 top reinforcement, and 6-mm diameter Grade 400 stirrups at 75 mm o/c. The shear reinforcements were over designed to prevent any premature shear failure. A 6-mm bar was placed 50 mm from the bottom of the specimen to serve as the cathode for the accelerated corrosion process.

Figure 1(b) shows the dimensions and reinforcement details of the large-specimens. The specimen had a cross-section of 152×254 mm and a total length of 3200 mm with a span of 3000 mm. Two No. 15 Grade 400 deformed rebars were used as the main bottom longitudinal reinforcement, and two 8 mm diameter plain rebars were used as the top reinforcement. Shear reinforcement were 8 mm diameter stirrups with 80 mm spacing. A stainless steel 16 mm diameter rebar was placed in the bottom third of each specimen to act as a cathode for the accelerated corrosion. A typical clear cover of 25 mm was used all round the stirrups.

To depassify the steel, the specimens were chloride-contaminated by premixing 2% chlorides by weight of cement in the bottom third of each specimen. Chlorides were placed over the whole length of the beam in the small-scale specimens but were concentrated in the flexure region in the large-scale specimens. The specimens were exposed to different corrosion levels (minor at 5%, moderate at 10% and severe at 15% mass loss) by means of a constant impressed current as described later. Strain gauges were placed on the FRP laminates to monitor and quantify tensile strains induced by the corrosion process. Following the corrosion phase, the specimens were tested in flexure in a four-point bending regime.

Material Properties

The specified 28-day compressive strength was 35 MPa with a maximum aggregate size of 19 mm, and w/c ratio of 0.6. The yield strength and the ultimate strength of the main reinforcing No.15 rebars were 445 MPa and 630 MPa, respectively. The Glass (GFRP) sheets used in large-scale beams had an ultimate strength of 600 MPa, an elasticity modulus of 26 GPa, and an ultimate elongation of 2.24%. The Carbon (CFRP) sheets used in large-scale beams had an ultimate strength of 960 MPa, an elasticity modulus of 73 GPa, and an ultimate elongation of 1.33%. The CFRP laminates used to strengthen the small-scale beams had a thickness of 0.11 mm (dry fibres), tensile strength of 2450 MPa, modulus of elasticity of 160 GPa, and ultimate elongation of 1.5%.

Accelerated Corrosion

Figure 2 shows a general view of the corrosion chamber. This chamber includes a steel rack to support the specimens and mist nozzles that mix pressurized air and water to create a mist (100% R.H.). Accelerated corrosion was applied using a constant impressed current with an approximate density of $150 \mu\text{A}/\text{cm}^2$. The current was impressed through the main longitudinal rebars, which act as the anode while the stainless steel bar in each specimen acts as the cathode. During accelerated corrosion, the specimens were subjected to wet-dry cycles to provide water and oxygen that are essential for the corrosion process.

FRP Repair Schemes

Specimens were either strengthened prior to corrosion or repaired after being corroded using different schemes of Carbon or Glass FRP sheets. The strengthening scheme used in the small-scale beams consisted of CFRP flexural laminate bonded to the tension face, with the fibre orientation in the longitudinal direction followed by transverse laminates bonded to the tension face and up each side of the beam, with the fibre orientation in the transverse direction. The transverse laminates fully anchor the flexural laminate along whole length of the beam and thus will prevent any premature delamination.

In the large-scale beams, prior to the application of the FRP sheets, longitudinal cracks due to corrosion were sealed using an epoxy adhesive. Then, FRP sheets were applied for repair where two repair schemes were chosen. The first scheme involved wrapping the specimen intermittently with U-shaped glass (GFRP) strips around the tension face and the sides. The second scheme involved flexural strengthening of the corroded specimen by externally bonding carbon (CFRP) sheet to the tension face of the specimen and then wrapping the specimen with U-shaped GFRP sheets. These repair schemes are illustrated in Figure 3.

Test Results and Discussion

Deterioration due to corrosion

By examining the corroded un-repaired large-scale specimens, some typical cracking patterns were identified; a) Pattern 1, where longitudinal cracks were located at the bottom soffit of the specimen, while no cracking appeared on both sides of the beam section, b) Pattern 2, where one longitudinal crack appeared at the bottom soffit of the specimen and the other crack appeared on one of the sides, c) Pattern 3, where longitudinal cracks appeared on the specimen sides, while no cracks were observed on the bottom soffit, and d) Pattern 4, where longitudinal cracks crossed over from the bottom soffit of the specimen to the sides and in some cases going back to the bottom soffit, which is a mix of the previous patterns. No spalling of concrete cover was observed. These cracking patterns are shown in Figure 4. The width of the longitudinal cracks was measured at discrete time periods throughout the accelerated corrosion process for all the corroded specimens. Figure 5 shows the average crack width versus mass loss for the corroded specimens.

The average longitudinal crack width before sealing of the corrosion cracks was 0.8 mm. When the repaired specimens were exposed to further corrosion, the sealed cracks did not open, and there was hardly any other longitudinal cracking observed. However, the 30mm long strain gauge mounted on the FRP sheet showed that by the end of the corrosion process, a strain of about 5000 $\mu\epsilon$ was measured for specimen (13-RI), which indicates an expansion of 0.15 mm of the longitudinal sealed crack. Up to 150 days after FRP repair, the longitudinal crack widened by only 0.15 mm, whereas for the un-repaired specimens, the longitudinal cracking widened by 1.2 mm to a final crack width of 2.0 mm. Figure 5 clearly shows that the FRP repair process reduced the crack opening by about 88% at the end of corrosion process. This implies a significant enhancement in appearance of FRP repaired corroded specimens by reducing crack opening due to further corrosion.

Effect of uniform corrosion on structural behaviour

The small-scale beams had uniform corrosion along the whole length of the specimen. The structural performance, with the exception of ductility, of the CFRP strengthened and corroded specimens was improved as shown in Figure 6 (a) and (b).

Figure 6a shows the behaviour of specimens strengthened with transverse CFRP wrapping only. The continuous transverse laminate provided a small increase in the yield and ultimate strength as a result of the transverse strength of the laminate. The transverse strength of cured uni-directional laminates is typically less than 10% of the longitudinal strength, but was sufficient in these specimens to increase the strengths by a significant amount. The difference in yield and ultimate load between N-0 and C-10 is small. Thus, the continuous transverse sheet was successful at maintaining the majority of the yield and ultimate strength of Specimen C-10. The yield and ultimate strengths of Specimen C-10 were 8% and 14% less, respectively, than the corresponding values for Specimen C-0. The loss in structural strength from Specimen C-0 to C-10, therefore, is approximately equal to the loss in steel cross-section.

Figure 6b shows the behaviour of specimens with transverse and flexural CFRP sheets. The tensile steel reinforcement of the strengthened specimens were corroded to 0% (CF-0), 5% (CF-5), 10% (CF-10) and 15% (CF-15) mass loss. The load-deflection response of the control beam (N-0) and the unstrengthened specimen corroded to 15% (N-15) are shown for comparison. All the strengthened beams exhibited increased stiffness over the unstrengthened specimens, and marked increases in the yield and ultimate strength. However, the ductility was reduced in comparison to unstrengthened uncorroded beam. The increase in yield and ultimate strength of the strengthened specimens were on average 24.5% and 50%, respectively. The percentage loss in yield and ultimate strength versus Specimen CF-0 was less than the percentage mass loss, due to the presence of the flexural sheet on the bottom of the beam. Comparison of the unstrengthened specimens (N15 vs N0) reveals that the corroded specimens exhibited deteriorated structural performance in comparison to the control-uncorroded specimen. It can be seen that the decrease in yield and ultimate strength is roughly proportional to the percentage mass loss.

The effects on the normalized yield strengths of specimens of the continuous transverse sheet and the longitudinal flexural sheet are shown in Figure 7. From 0% mass loss to 10% mass loss, approximately 25% of the increase in yield strength between the N-series of specimens and the CF-series is provided by the continuous transverse sheet, and the remainder is provided by the flexural sheet. The yield strengths of Specimens C-S-10 and C-10 were almost identical, as were the yield strengths of Specimens CF-S-0 and CF-0. The yield strength of Specimen CF-S-10 was only 3% greater than the yield strength of Specimen CF-10. Thus, the presence of stirrups did not have any significant effect on the yield strength of the specimens. Specimens IF-10 and CF-R exhibited normalized yield strengths, which were 2%, less than the normalized strength of Specimen CF-10.

The effects of the continuous transverse sheet and longitudinal flexural sheet on the normalized ultimate strengths of specimens are shown in Figure 8. On average, 20% of the difference in ultimate strength can be attributed to the continuous transverse sheet, with the remaining 80% due to the flexural sheet. The ultimate strengths of the CF series were about 45% higher than the corresponding strengths of the N-series and the ultimate strengths of the C-series were about 10% larger than those of the N-series at different corrosion levels. The effect of the stirrups on the ultimate strength between the CF-series and CF-S series is labelled as well. The stirrups acted to confine the concrete in compression, thereby allowing a higher concrete strain at failure in the CF-series than the concrete strain at failure in the CF-S series. This higher strain resulted in a larger ultimate load. The increase in ultimate strength afforded by the stirrups was

approximately 40% of the increase in strength afforded by the continuous transverse sheet. In Figure 9, it can be seen that the ultimate strengths of the N-series of specimens decreased on average 25% faster than the ultimate strengths of the CF-series as the rate of corrosion increased. This is a similar pattern to the yield strengths plotted in Figure 8. Again, the lower rate of strength loss in the CF-series is a result of the longitudinal flexural laminate that was not affected by corrosion.

Effect of corrosion within flexural zone on structural performance

Figure 9 shows the measured load-deflection response of the specimens repaired using GFRP U-wrapping + CFRP flexural sheets - scheme II (11-RII, 12-RII, and 13-RII) together with the predicted performance of a virgin specimen strengthened using the same scheme (referred to as 00-RII-Analytical). In general, compared to the corroded un-repaired specimens, the performance was greatly enhanced due to the addition of the CFRP flexural sheet in spite of the high corrosion experienced by the main rebars. The yield load increased by an average of 21%, and the ultimate load increased by an average of 28%. The effects of corrosion on the flexural behaviour were: The yield load of corroded strengthened specimens was reduced by 1%, 3%, and 3% at 5.5%, 9%, and 10.5% mass loss, respectively compared to the un-corroded strengthened specimen. On the other hand, the ultimate capacity was reduced by 4.2%, 2.1%, and 2.3% at 5.5%, 9%, and 10.5% mass loss, respectively compared to the un-corroded strengthened specimen. Figure 10 shows the reduction percent for the yield and the ultimate loads for these specimens due to corrosion, together with the corroded un-repaired specimens. This figure shows that the yield load was reduced by 1%, 3%, and 3% at 5.5%, 9%, and 10.5% mass loss, respectively compared to the un-corroded strengthened specimen (00-RII). On the same figure, the anticipated performance for the repaired specimens if they were not exposed to further corrosion after repair (short-term performance), is shown. This anticipated performance was predicted based on the performance of the corroded un-repaired specimens. According to this anticipated performance, it can be shown that the post-repair performance was not enhanced at 9% mass loss, but the yield load increased by about 1% at 10.5% mass loss, and at least 2.5% at 12.5% mass loss. This figure also shows that the ultimate capacity was reduced by 4.2%, 2.1%, and 2.3% at 5.5%, 9%, and 10.5% mass loss, respectively compared to the un-corroded strengthened specimen (00-RII). This figure also the anticipated performance for the ultimate load for the repaired specimens if they were not exposed to further corrosion after repair, which was predicted based on the performance of the corroded un-repaired specimens. According to this anticipated performance, it can be shown that the post-repair performance was enhanced since the ultimate loads increased by about 3.3% at 9% mass loss, 4% at 10.5% mass loss, and at least 6% at 12.5% mass loss.

Conclusion

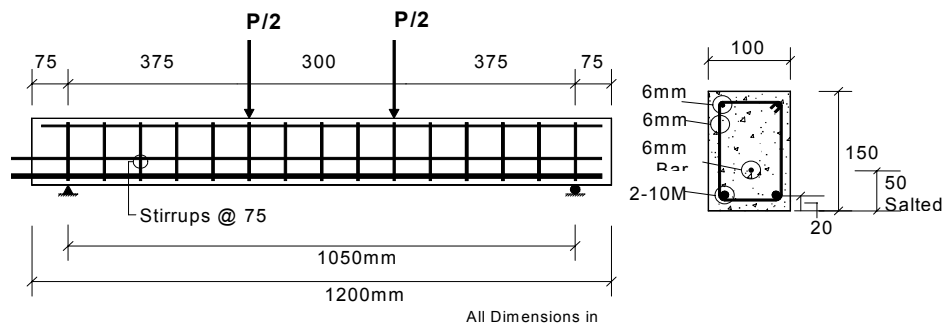
This study revealed that FRP composites for strengthening or repair of reinforced concrete beams that are experiencing steel reinforcement corrosion are capable to maintain the structural integrity, serviceability and ultimate monotonic strength. Future work will investigate the FRP repair of corrosion-damaged concrete specimens which is more realistic of field conditions. The results in this paper provided important benchmark data.

Acknowledgements

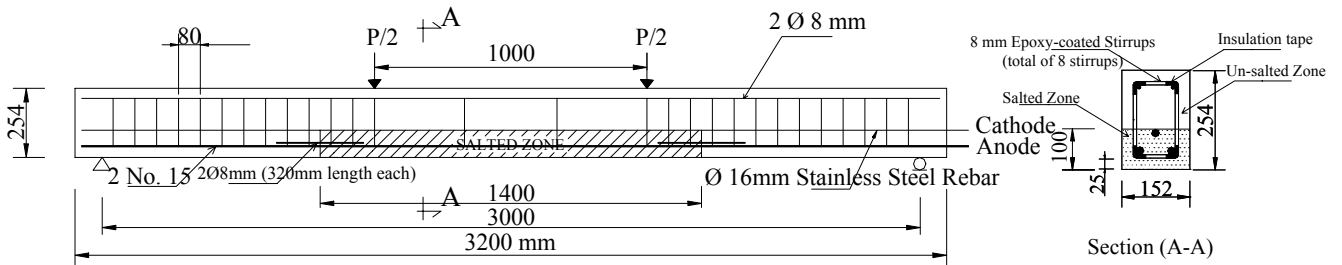
The author is a project leader in the Intelligent Sensing for Innovative Structures Network and wishes to acknowledge the support of the Network of Centres of Excellence Program of the Government of Canada and the Natural Sciences and Engineering Research Council of Canada.

References

1. ACI Committee 222. (1996). Corrosion of Metals in Concrete, ACI 222R-96, American Concrete Institute, Detroit, Michigan, 29 pp.
2. ACI Committee 440. (1996). State of the Art Report on Fiber Reinforced Plastic Reinforcement for Concrete Structures, ACI 440R-96, American Concrete Institute, Detroit, Michigan, 68 pp.
3. Masoud, S. and Soudki, K.A., (2000). Serviceability of Corroded Carbon Fibre Reinforced Polymer Strengthened Reinforced Concrete Beams, *Proceedings of 3rd Structural Speciality Conference of the Canadian Society for Civil Engineering*, London, June, pp. 507-514.
4. Masoud, S. and Soudki, K.A., (2001). Rehabilitation of Corrosion-Damaged Reinforced Concrete Beams with CFRP Sheets, International Conference on FRP Composites in Civil Engineering, 12-14 December, Hong Kong, Elsevier, pp. 1617-1624.
5. Sherwood, T. and Soudki, K.A., (1998). Durability of Concrete Beams Repaired with Carbon Fibre Reinforced Polymer Laminates Subjected to Accelerated Rebar Corrosion, *CSCE Annual Conference*, Vol. III, Halifax, June, pp. 663-672.
6. Sherwood, T. and Soudki, K.A. (1999). Confinement of Corrosion Cracking in Reinforced Concrete Beams with Carbon Fibre Reinforced Polymer Laminates, ACI-SP-188 on Non-Metallic (FRP) Reinforcement for Concrete, pp. 591-603.
7. Sherwood, E.G. and Soudki, K.A., (2000). Rehabilitation of Corrosion Damaged Concrete Beams with CFRP Laminates- Pilot Study, *Composites Part B: Engineering*, Vol. 31, pp. 453-459.
8. Soudki, K.A. and Sherwood, T., (1998). Repair of Corroded RC Beams with Carbon FRP Sheets, 5th *International Conference on Composites Engineering*, Las Vegas, July 5-11, pp 819-820.
9. Soudki, K.A., (1999). Effects of CFRP Wrapping on the Bond Strength of Corroded Steel Reinforcing Bars, *American Concrete Institute Spring Convention*, Chicago, March.
10. Soudki, K.A. and Sherwood, T., (2000). Behaviour of Reinforced Concrete Beams Strengthened with CFRP Laminates Subjected to Corrosion Damage, *Canadian Journal of Civil Engineering*, Vol. 27, No. 5, pp 1005-1010.
11. Soudki, K.A., Craig, B. El-Salakawy, E., (2000). "Behavior of CFRP Strengthened Reinforced Concrete Subjected to Corrosive Environment," *American Concrete Institute Fall Convention*, Toronto, October.



(a)



(b)

Figure 1. Beam dimensions and reinforcements for a) small-, b) large-scale specimens



Figure 2. Specimens in the corrosion chamber

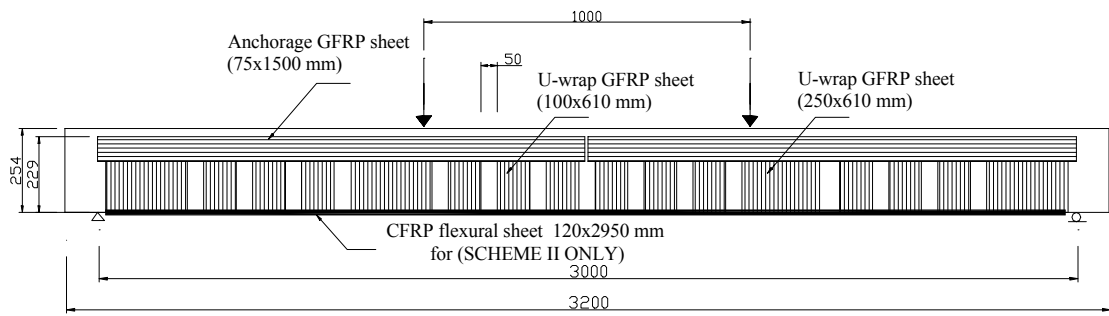


Figure 3. FRP repair schemes

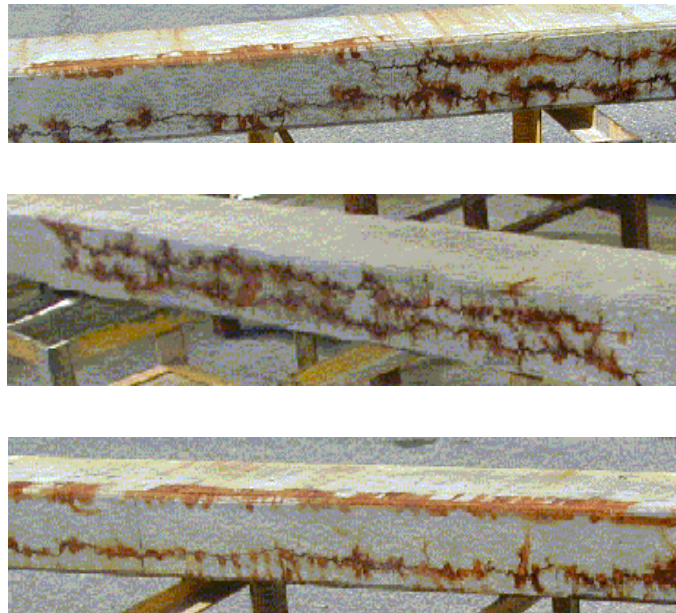


Figure 4. Corrosion cracking pattern in large-scale specimens

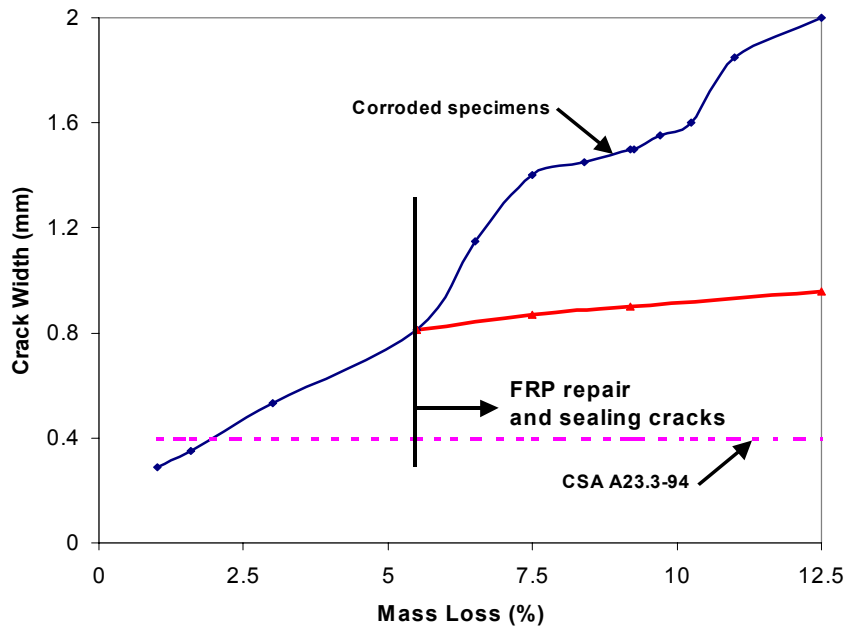


Figure 5. Crack width vs. mass loss

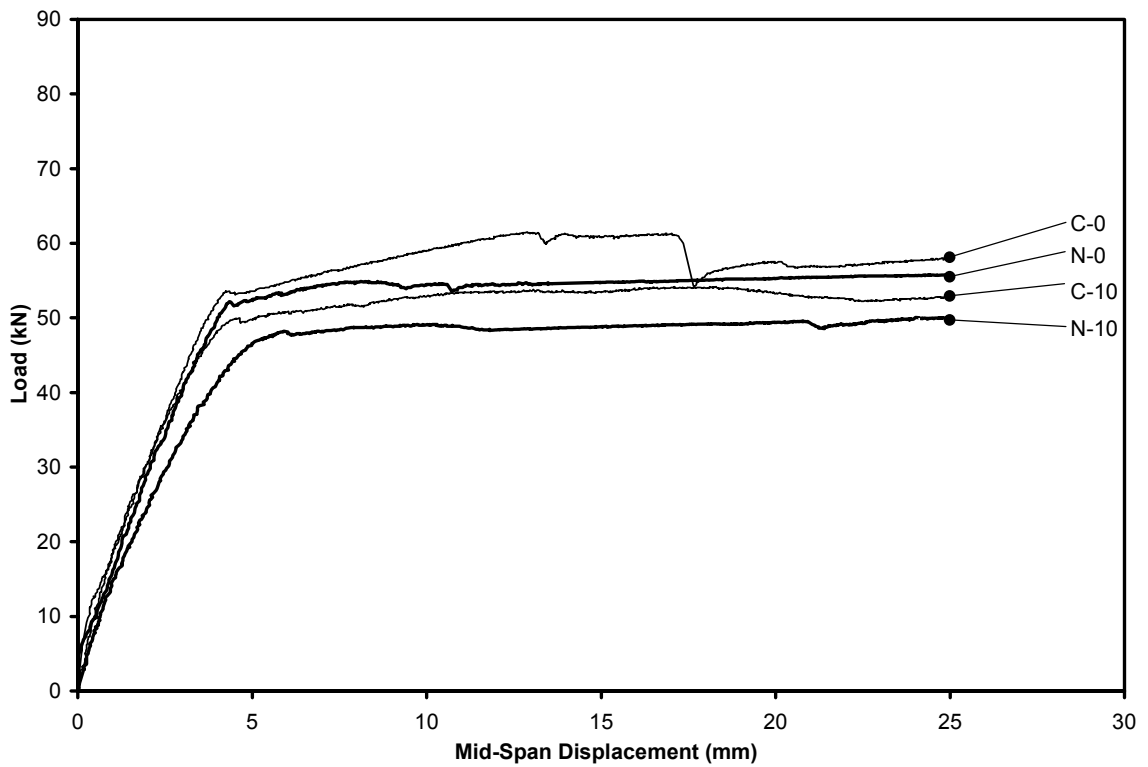


Figure 6a. Behaviour of small-scale CFRP strengthened RC beams at different corrosion levels

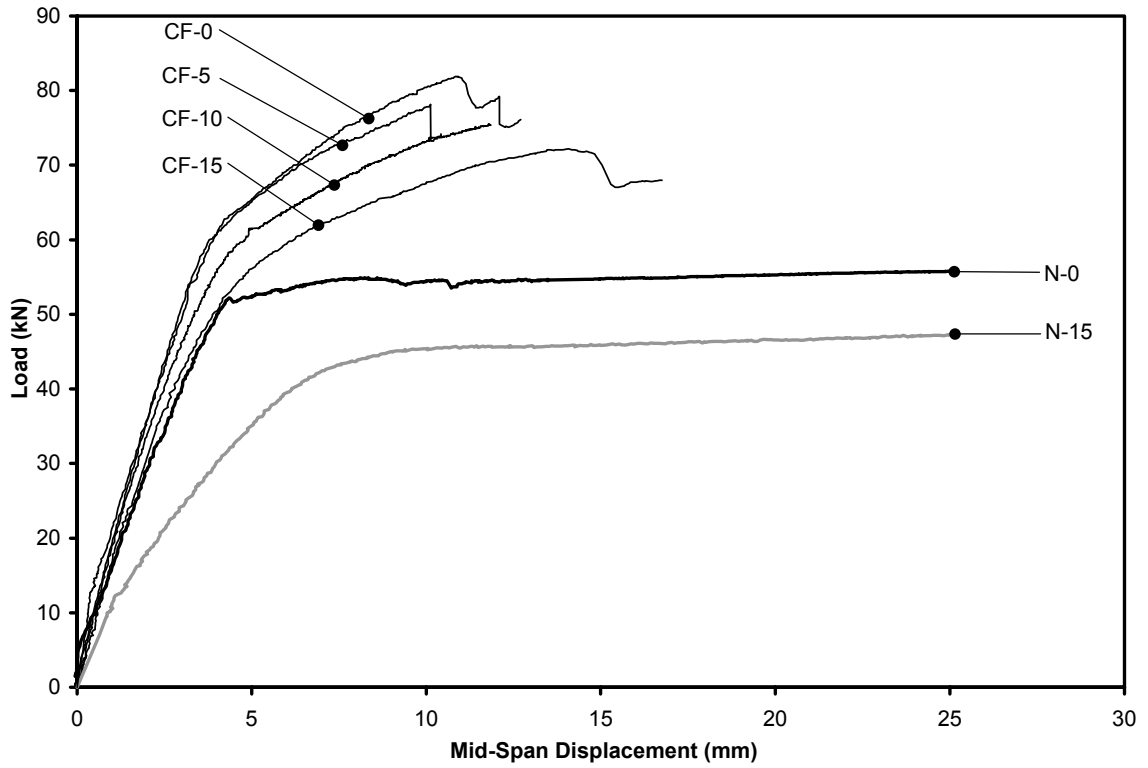


Figure 6b. Behaviour of small-scale CFRP strengthened RC beams at different corrosion levels

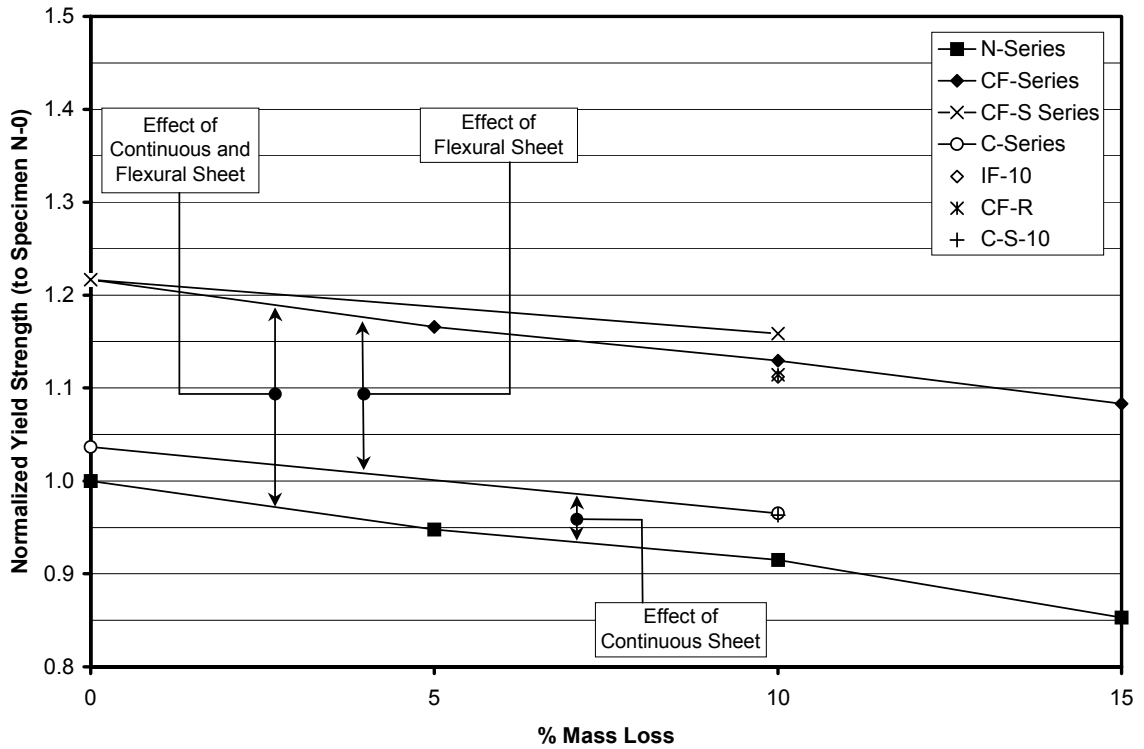


Figure 7. Small-scale specimens - normalized yield strength (to specimen N-0) vs. % mass loss

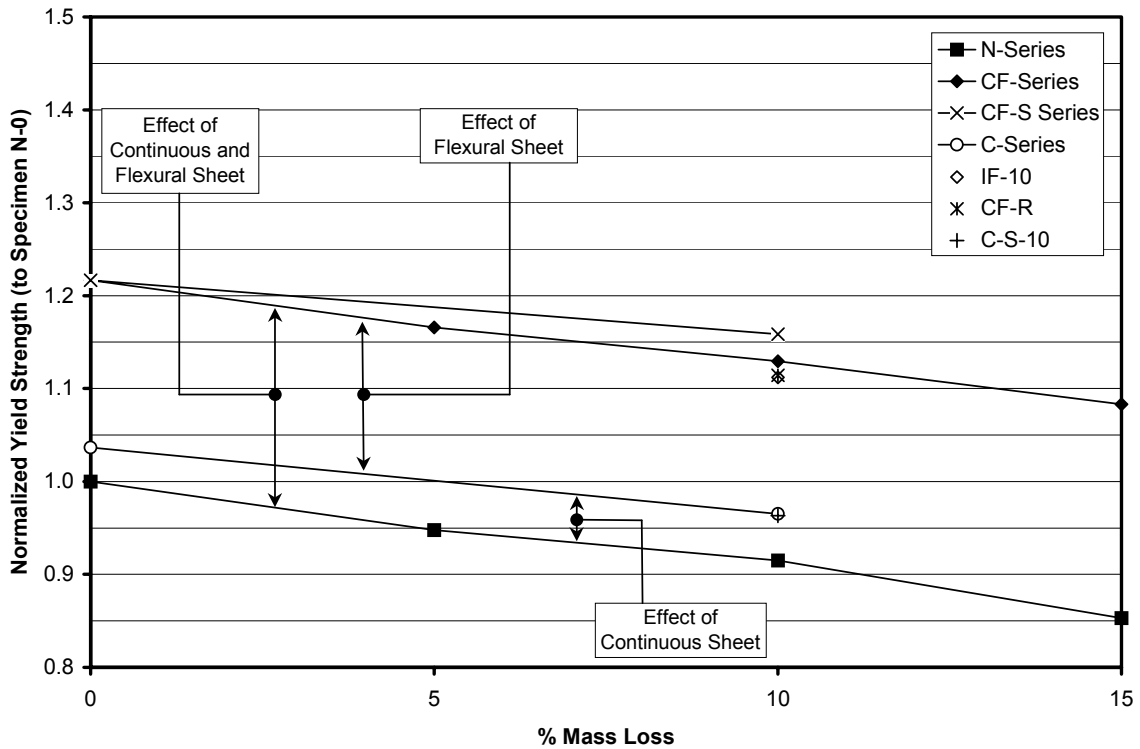


Figure 8. Small-scale specimens - normalized ultimate strength (to specimen N-0) vs. % mass loss

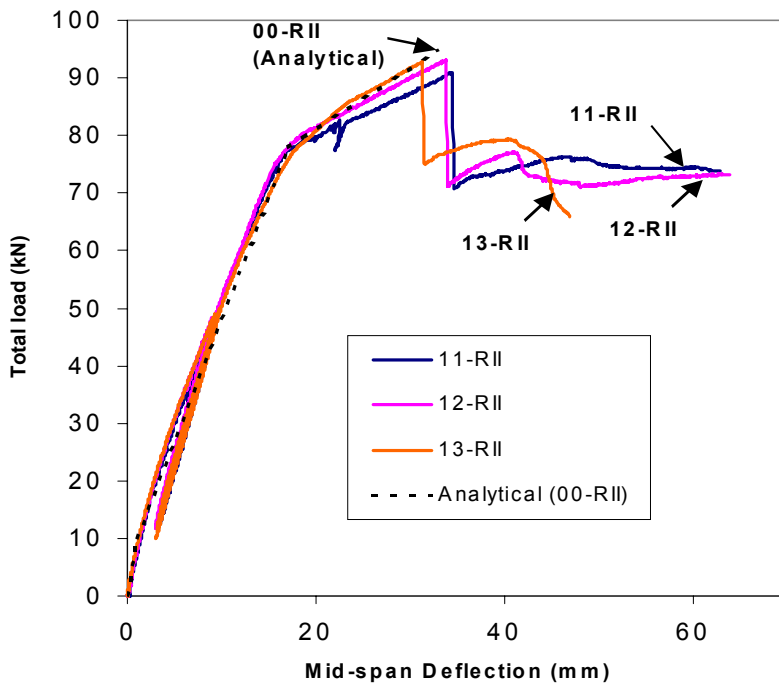


Figure 9. Behaviour of large-scale specimens repaired with GFRP U-wraps and CFRP flexural sheets

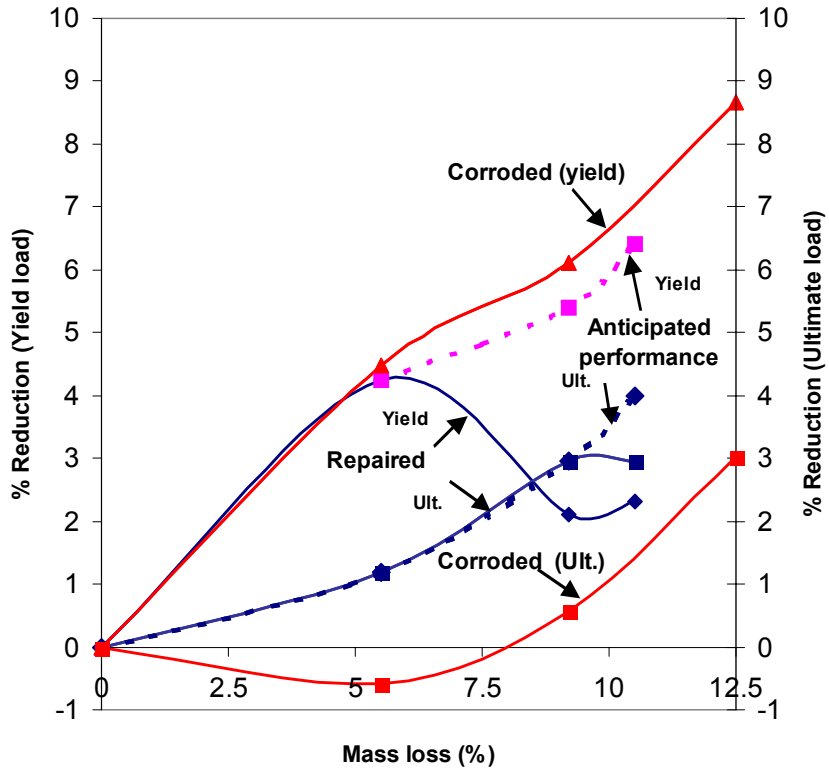


Figure 10. Large-scale specimens - % reduction in yield and ultimate load vs. mass loss